Articles

Denaturation of Human Cu/Zn Superoxide Dismutase by Guanidine Hydrochloride: A Dynamic Fluorescence Study†

Giampiero Mei,‡ Nicola Rosato,‡ Norberto Silva, Jr.,§ Ruth Rusch,§ Enrico Gratton,§ Isabella Savini,‡ and Alessandro Finazzi-Agrò*,‡

Dipartimento di Medicina Sperimentale e Scienze Biochimiche, Università di Roma "Tor Vergata", Via O. Raimondo 8, 00173 Rome, Italy, and Laboratory for Fluorescence Dynamics, Department of Physics, University of Illinois at Urbana—Champaign, 1110 West Green Street, Urbana, Illinois 61801

Received November 19, 1991; Revised Manuscript Received May 12, 1991

ABSTRACT: The unfolding of holo and apo forms of human Cu/Zn superoxide dismutase by guanidine hydrochloride has been investigated by steady-state and dynamic fluorescence. In agreement with previous observations, a stabilizing effect of the metal ions on the protein tertiary structure was apparent from comparison of apo- and holoproteins, which both showed a sharp sigmoidal transition though at different denaturant concentrations. The transition was also followed by circular dichroism to check the extent of secondary structure present at each denaturant concentration. The results are incompatible with a simple two-state mechanism for denaturation. The occurrence of a more complicated process is supported by the emission decay properties of the single tryptophanyl residue at different denaturant concentrations. A complex decay function, namely, two discrete exponentials or a continuous distribution of lifetimes, was always required to fit the data. In particular, the width of the lifetime distribution, which is maximum at the transition midpoint, reflects heterogeneity of the tryptophan microenvironment and thus the presence of different species along the denaturation pathway. In the unfolded state, the width of the lifetime distribution is broader than in the folded state probably because the tryptophan residue is affected by a larger number of local conformations. The dissociation of the dimer was also studied by varying the protein concentration at different denaturant concentrations. This process affects primarly the surface of the protein rather than its secondary structure as shown by a comparison between the tryptophan emission decay and circular dichroism data under the same conditions. Another consequence of dissociation is a greater instability in the structure of the monomers, which are more easily unfolded. This finding lends support to the idea that the quaternary structure is crucial for the stability of oligomeric proteins.

The stability of globular proteins is a relevant problem in biophysics. The analysis of the denaturation curves obtained using various denaturing agents (urea, guanidine, heat, acids, pressure) and different techniques (circular dichroism, calorimetry, fluorescence, nuclear magnetic resonance) (Pace, 1986) is useful to investigate the chemical and physical properties of the folded and unfolded states and hence to get information about the mechanism of folding (Creighton, 1978). Recently it was suggested that the classical two-state theory of unfolding for small globular proteins is not appropriate to describe the process of denaturation and a new general "stepwise" mechanism for protein folding was proposed (Kim & Baldwin, 1982; Ptitsyn et al., 1990; Jaenicke, 1991).

As a matter of fact, the presence of stable structural intermediate(s) between the native and the unfolded state has been revealed and characterized with various methodologies for at least three different proteins (Kuwajima, 1977; Dolgikh et al., 1981, 1984; Holladay et al., 1974). It was pointed out that relevant volume and surface effects, which characterize these intermediate species, are taking place during the unfolding transition. In the case of oligomeric proteins, however, the mechanism of unfolding is even more complicated because monomerization can occur. In particular, it would be interesting to know if the two processes take place at the same time. Knowledge of these details will bring important information about protein stability.

Time-resolved fluorescence spectroscopy and anisotropy decay studies are well-established methods to characterize the conformational transition occurring during the unfolding process. Furthermore, fluorescence lifetimes and rotational correlation times of intrinsic probes, like tryptophan or tyrosine residues, belong to the same time scale of local protein motions and fluctuations (Beechem & Brand, 1985; Weber, 1953; Karplus & Petsko, 1990). Thus, a description of processes involving the dynamics of the microenvironment of the fluorophore as well as those concerning the protein as a whole is accessible using dynamic fluorescence methods. Traditionally, the fluorescence intensity decays were analyzed using a sum of discrete exponentials. This model was generally interpreted by assuming that different discrete species are simultaneously present in solution. Recent improvements in technology and in computer analysis have suggested the possibility of describing protein fluorescence decay using continuous distributions of lifetimes (Alcala et al., 1987a,b,c; Libertini & Small, 1989). This approach has already been used in the case of apomyoglobin (Bismuto et al., 1988) and

† The LFD members are supported by the Division of Research Resources of the National Institutes of Health (PHS-P41-5-RR03155) and by UIUC. This work was also supported by Italian National Research Council (CNR), Target project "Biotechnology and Bioinstrumentation".

* To whom correspondence should be addressed.
‡ Università di Roma "Tor Vergata".
§ University of Illinois at Urbana—Champaign.

0006-2960/92/0431-7224$03.00/0 © 1992 American Chemical Society

human superoxide dismutase (Rosato et al., 1990a,b) to explain the effect of temperature on the protein subconformations. It has been found that the width of the lifetime distribution increases upon denaturation and that the distribution width can be used as an indicator of the number of protein conformations. On the other hand, the distribution analysis failed in describing the unfolding of ribonuclease T_1 by temperature and guanidine hydrochloride (GdHCl)[1] (Gryczynski et al., 1988). However, it should be noted that the properties of the tryptophan in native ribonuclease T_1 are completely different from those of the same probe in the other two proteins. In fact, in ribonuclease T_1, it is buried inside the protein in a highly hydrophobic region that provides the conditions for a homogeneous fluorescence decay. Furthermore, anisotropy decay measurements showed that this tryptophan residue is immobile at room temperature (James et al., 1985). These examples clearly show that the adequacy of discrete or continuous decay models is related to the specific chemicophysical properties of the sample under scrutiny.

In this paper, we have studied the GdHCl-induced unfolding of HSOD, a dimeric protein composed of two identical subunits, each containing a single tryptophan residue exposed to the solvent. The stability of a cognate protein, bovine superoxide dismutase, in the presence of 8.0 M urea (Malinowski & Fridovich, 1979) and SDS (Forman & Fridovich, 1973) has already been reported. The conformational stability of the enzyme seems to be a common feature of all Cu/Zn SODs, which have large structural homology (Getzoff et al., 1989).

To investigate the unfolding mechanism of HSOD, we have measured the steady-state and time-resolved intrinsic fluorescence as a function of GdHCl concentration. The fluorescence decay of this protein has been fitted with a continuous distribution of lifetimes or with a sum of two discrete exponentials. A comparison between the two models is reported and discussed in terms of mathematical, statistical, and physical considerations. In addition, steady-state anisotropy and anisotropy decay data have been collected at different denaturation stages. The structural transition was also followed by circular dichroism. All these data give new information about the stability and denaturation mechanism of HSOD. Altogether, they qualify time-resolved fluorescence as a valuable method for identification of metastable protein conformers.

MATERIALS AND METHODS

Sample Preparation. HSOD was purified from human erythrocytes (Bannister & Bannister, 1984). Metal-depleted HSOD was prepared by dialyzing the protein against 1 mM EDTA in 0.05 M sodium acetate buffer, pH 3.5, for 24 h and then for 12 h at pH 7.6. The samples used for fluorescence experiments were dissolved in 0.01 M potassium phosphate buffer, pH 7.6. For denaturation experiments, each sample was prepared by diluting 0.3 mL of protein stock solution to 2 mL with GdHCl-containing buffer. All measurements were carried out at 20 °C after 20-h incubation in the presence of GdHCl at 4 °C. Ultrapure GdHCl was purchased from United States Biochemical and tested for purity in spectral absorption and fluorescence.

Fluorescence Measurements. Protein unfolding curves were recorded by measuring the steady-state intrinsic fluorescence and the fluorescence polarization at various concentrations of GdHCl using a single-photon-counting (ISS, Inc., Champaign, IL; Model GREG PC) or a Jobin–Yvon Model 3D spectrofluorometer.

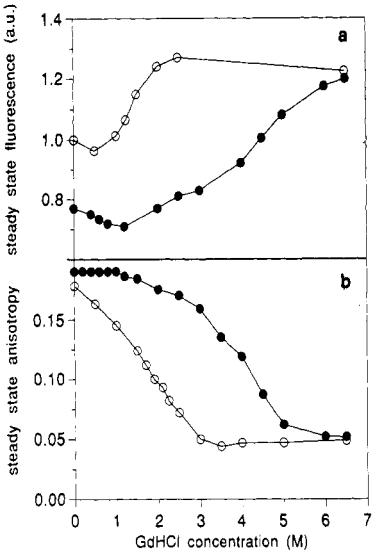

FIGURE 1: Dependence of fluorescence intensity (a) and steady-state anisotropy (b) on GdHCl concentration for holo-HSOD (filled symbols) and apo-HSOD (open symbols).

Frequency domain techniques were used to measure the intrinsic fluorescence decay and the fluorescence depolarization of the protein in the range 10–240 MHz (Gratton et al., 1984). The light source was a high-repetition mode-locked Nd–Yag laser, and the harmonic content of the laser was used as previously described (Gratton & Linkeman, 1983). Excitation was at 295 nm (through a polarizer oriented at the "magic angle") while emission was observed through a WG335 cutoff filter to remove scattered light. Data analysis was performed by minimizing the reduced χ^2 with a routine based on the Marquardt algorithm using the Globals Unlimited software (Beechem & Gratton, 1988).

Except for dissociation measurements, all fluorescence experiments were performed using samples in the absorbance range 0.04–0.10 at 295 nm. The experiments at high concentration were performed using special cuvettes (3 × 3 mm) with two dark faces to avoid multiple reflection.

Circular Dichroism Measurements. Circular dichroism measurements were carried out using a Jobin–Yvon CD VI spectropolarimeter. The sample holder was thermostated at 20 °C using an external bath circulator. All samples were in the concentration range 0.1–1.0 mg/mL, and the measurements were performed in 1.0-cm quartz cuvettes.

Analytical Ultracentrifugation. Sedimentation velocity experiments were carried out at 10 °C and 52 000 rpm on a Spinco Model E ultracentrifuge equipped with a temperaturecontrol unit. Protein concentrations were varied between 4.8 and 5.3 mg/mL. The sedimentation coefficients were evaluated from the maximum ordinate of the schlieren peak and were reduced to $s_{20,w}$ by standard procedures.

RESULTS

Steady-State Measurements. Fluorescence emission spectra of native and metal-depleted HSOD have already been reported (Rosato et al., 1990b). Both spectra are structureless, centered at 344 nm, and essentially similar to that of *N*-acetyltryptophanamide in the same buffer. Their intensity is reported in Figure 1a as a function of GdHCl concentration. Figure 1b shows the steady-state fluorescence anisotropy of

[1] Abbreviations: CD, circular dichroism; HSOD, human superoxide dismutase; GdHCl, guanidine hydrochloride; SDS, sodium dodecyl sulfate; EDTA, ethylenediaminetetraacetic acid; DTT, dithiothreitol.

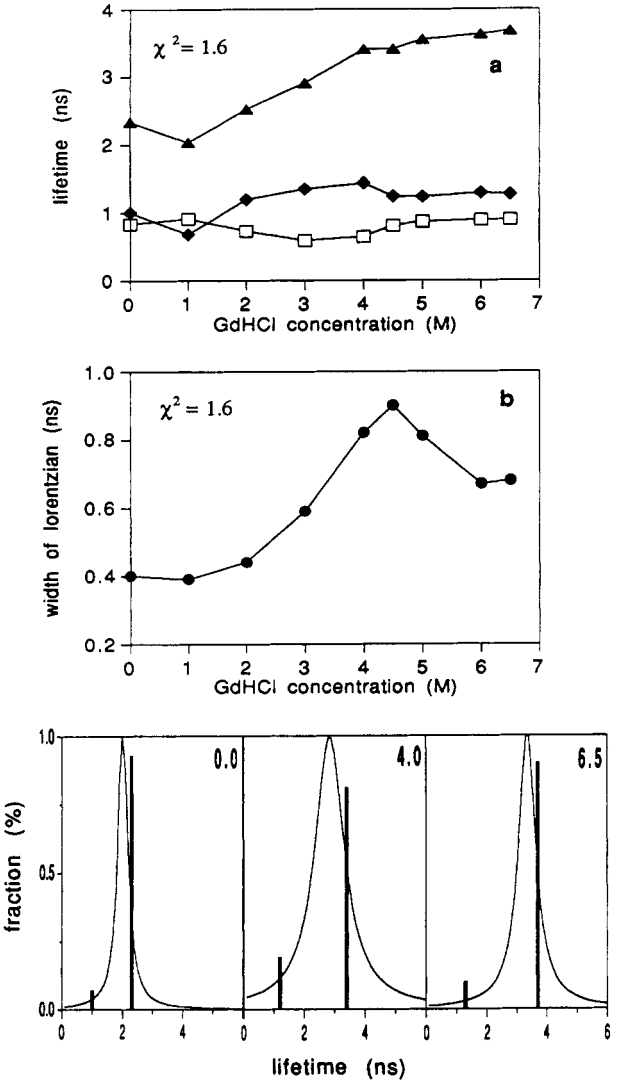

FIGURE 2: (a) Dependence of the fluorescence lifetime (filled symbols) and its long component fraction (open symbols) on GdHCl concentration: discrete lifetimes model. (b) Dependence of the width of the Lorentzian function on denaturant concentration: continuous distribution of lifetimes model. Bottom: comparison of the discrete and distributed lifetime models at 0.0, 4.0, and 6.5 M GdHCl concentration. The values of χ^2 reported in (a) and (b) correspond to the best global fit obtained with each model.

the same samples. The anisotropy for *N*-acetyltryptophanamide in buffer was $r = 0.003 \pm 0.001$. According to the anisotropy data, holo- and apoprotein forms are completely unfolded by GdHCl at 6.0 and 3.0 M, respectively, indicating a significant stabilizing effect of the metal ions.

Time-Resolved Fluorescence. Fluorescence decay data, obtained using frequency domain techniques, were fitted using different models, namely, one- and two-exponential functions or a continuous distribution of lifetimes (Rosato et al., 1990a,b). By comparison of the χ^2 values and of the pattern of weighted residuals in the different fits, it was again found that the fluorescence decay of the HSOD samples always requires a complex fit. From the point of view of statistics, the simplest satisfactory fit is the unimodal distributed Lorentzian lifetime model (Rosato et al., 1990a,b). In fact, it requires only two independent parameters (center and width) while three parameters are used for a double-exponential function (two lifetimes values and the relative fraction). Both methods were used to fit the fluorescence decays of HSOD at various GdHCl concentrations. Figure 2a,b shows the results obtained according to the two models. The bottom part of Figure 2

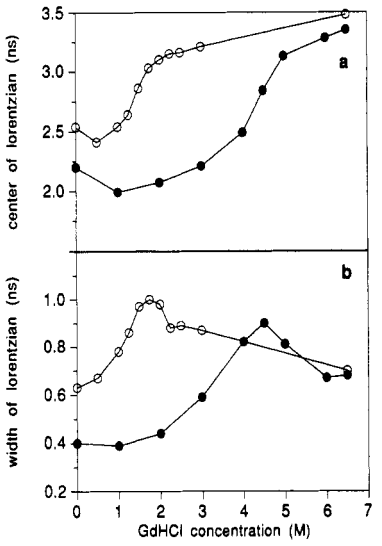

FIGURE 3: Dependence of the Lorentzian distribution center (a) and width (b) on GdHCl concentration for holo-HSOD (filled symbols) and apo-HSOD (open symbols).

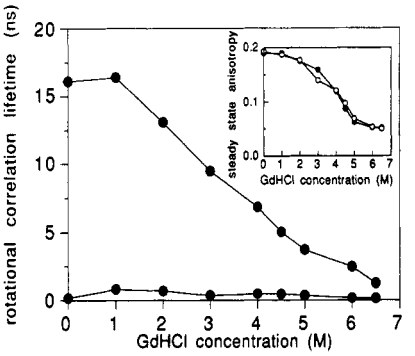

FIGURE 4: Rotational correlation times of holo-HSOD measured as a function of GdHCl concentration. Inset: experimental (filled symbols) and calculated (open symbols) steady-state fluorescence anisotropy of holo-HSOD as a function of GdHCl concentration. The steady-state anysotropy was calculated on the basis of the dynamic anysotropy values shown in the main panel.

shows that mathematically they are quite equivalent. In fact, the width of the distribution increases whenever the ratio of the relative fractions of the two discrete lifetimes decreases. As the χ^2 value is not improved by adding a new parameter, we adopted the continuous lifetime distribution model in the interpretation of the data. Furthermore, while the presence of two discrete lifetimes in the native protein is tenable, in the denatured samples it would require the presence of a contaminant species. Figure 3a shows the variation of the lifetime distribution center as a function of the denaturant concentration. Sigmoidal transition curves as a function of GdHCl concentration are observed for both protein forms. The dependence of the distribution width on the GdHCl concentration is shown in Figure 3b.

Anisotropy Decay Measurements. The anisotropy decay of HSOD has been measured at different points of the unfolding curve. At least two rotational correlation times were required to fit the data for both native and GdHCl-treated samples (Figure 4). Native HSOD shows a long rotational component of 15.9 ns and a short component of 0.09 ns. The slow rotation is compatible with the tumbling of a molecule of M_r 33 000. The calculated rotational lifetime for an equivalent rigid sphere would be 13 ns, while HSOD is in fact a prolate ellipsoid. The short component is in the range expected for local, fast rotation of the indolyl side chain

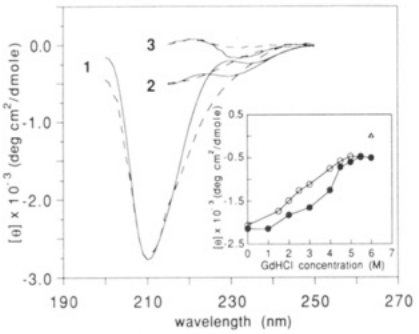

FIGURE 5: CD spectra for holo-HSOD (solid lines) and apo-HSOD (dashed lines) in 0.0 M GdHCl (1), 5.5 M GdHCl (2), and 6.0 M GdHCl plus DTT (3). Inset: CD intensity at 215 nm for holo-HSOD (filled symbols) and apo-HSOD (open symbols) as a function of GdHCl concentration. The triangle (Δ) corresponds to the samples in 6.0 M GdHCl plus DTT.

(Munro et al., 1979). The rotational rates obtained from anisotropy decay measurements were used to calculate the steady-state fluorescence anisotropy of holo-HSOD as a function of GdHCl concentration. The close agreement of calculated and observed values of the steady-state anisotropy is shown in the inset of Figure 4. It should be noted that at high denaturant concentration the two rotational times approach each other, making the attribution of each species less certain.

Circular Dichroism Experiments. CD spectra of HSOD between 200 and 250 nm were recorded at different GdHCl concentrations. Apo-HSOD has a broader spectrum and does not contain the copper-related peak at ≈230 nm. The data show that holo- and apoprotein samples show a residual dichroism even at 6.0 and 5.0 M GdHCl, respectively. This is probably due to the disulfide bond present in each subunit since the signal is completely lost upon addition of DTT (final concentration ≈ 1 mM) (Figure 5).

Analytical Ultracentrifugation. Native and 3.5 M GdHCl-treated HSOD samples were run in an analytical ultracentrifuge to monitor the quaternary structure during unfolding. Both native apo-HSOD and holo-HSOD in 10 mM phosphate buffer, pH 7.6, at ≈11 °C sediment as a single peak (Figure 6, top panel) of 2.48 and 2.88 S, respectively, as expected for their molecular weight value (≈33 000). No evidence for higher aggregates was found.

The sedimentation velocity pattern of the holoprotein in 3.5 M GdHCl shows instead a very broad peak sedimenting faster than that of apo-HSOD at the same denaturant concentration (Figure 6, bottom panel). Even though a thorough correction for the viscosity was not attempted, apo-HSOD seems to be completely dissociated into largely denatured subunits not sedimenting at this velocity and solvent viscosity, while holo-HSOD still sediments as an heterogeneous peak in which both monomeric and dimeric protein molecules are probably present.

Kinetics of HSOD Denaturation. The kinetics of HSOD denaturation were studied by mixing rapidly (≈5 s) the protein with GdHCl to final concentration of 6.5 M following the fluorescence change with time (Figure 7, dotted line). Attempts to fit these data with one- or two-exponential (continuous line) equations were not satisfactory as shown by the respective weighted residuals (Figure 7).

A mathematically better fitting was only obtained using a physically meaningless three-exponential equation (not shown). Qualitatively similar results were obtained at 3.5 M GdHCl. Altogether, these data rule out a simple one-step and even a two-steps process for the denaturation of HSOD.

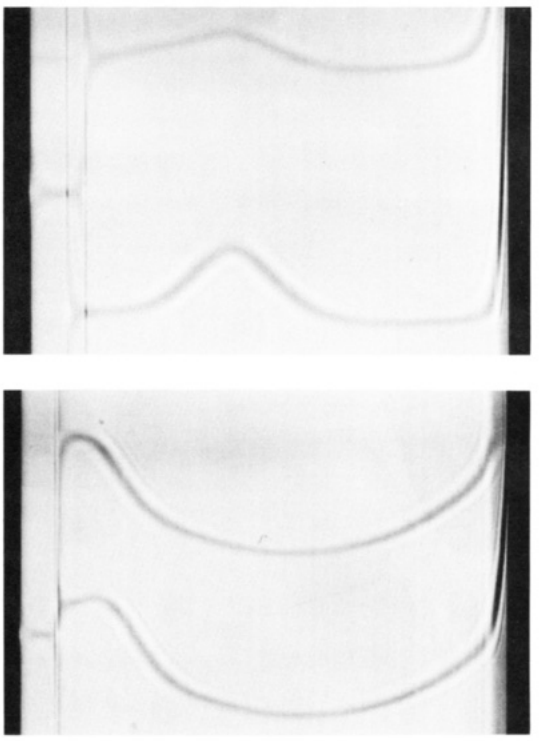

FIGURE 6: (Top) Sedimentation patterns of apo-HSOD (top curve) and holo-HSOD (bottom curve) in 10 mM phosphate buffer, pH 7.6 at 11 °C. (Bottom) Sedimentation patterns of apo-HSOD (top curve) and holo-HSOD (bottom curve) in 3.5 M GdHCl (same condition as in top panel). Photographs taken 179 (top panel) and 100 min (bottom panel) after reaching full speed (52 000 rpm). The sedimentation direction was from left to right.

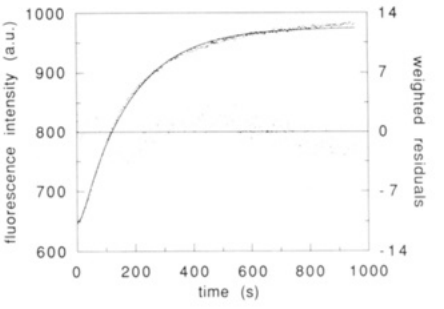

FIGURE 7: Kinetics of HSOD denaturation is 6.5 M GdHCl. The solid line represents a fit for a two-exponential model: $F(t) = 32.6e^{-0.086t} - 356.3e^{-0.006t} + 975.1$ ($\chi^2 = 3.5$). In the central part of the figure, the weighted residuals relative to the fit are shown.

Monomerization of HSOD. In order to test for the presence of a monomer–dimer equilibrium, suggested by analytical ultracentrifugation experiments, spectroscopic data were taken at different protein concentrations. The steady-state anisotropy and CD signal at 215 nm of holo-HSOD in 3.5 M GdHCl as a function of protein concentration are reported in Figure 8. The span of concentrations was ≈300 times. The data clearly show that monomerization is occurring without any change in the secondary structure of the protein as the anisotropy drops dramatically while the CD signal is constant over the concentrations studied. The anisotropy data were fitted using a simple two-state model (solid line) following the equilibrium reaction:

$$[D] \leftrightarrow 2[M]$$

Using a Marquardt algorithm and a value of the dimer steady-state anysotropy $r_d = 0.190 \pm 0.002$ (see Figure 1b), the dissociation constant at 3.5 M GdHCl was calculated to be 41 ± 8 μM. The asymptotic value at low protein

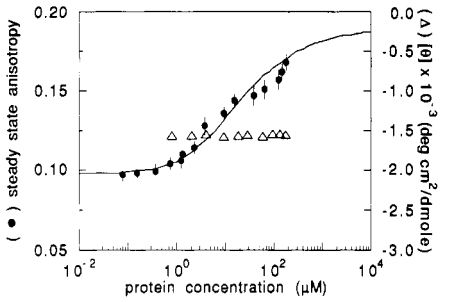

FIGURE 8: Steady-state anisotropy (●) and the CD signal at 315 nm (△) of holo-HSOD in 3.5 M GdHCl as a function of protein concentration. The solid line corresponds to the best fit ($\chi^2 \approx 1.1$) obtained using a simple monomer–dimer equilibrium.

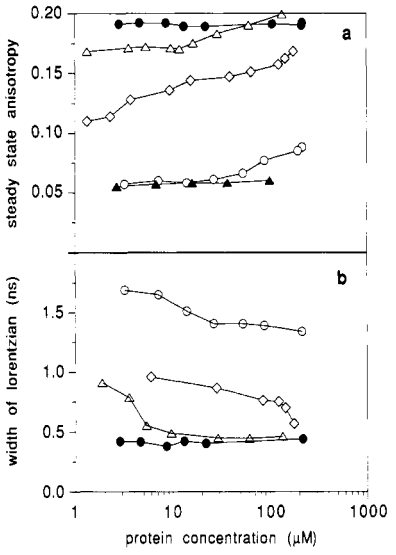

FIGURE 9: Steady-state anisotropy (a) and width of the Lorentzian distribution (b) of holo-HSOD as a function of protein concentration in the presence of 0.0 (●), 2.0 (△), 3.5 (◇), 5.0 (○), and 6.5 M (▲) GdHCl.

concentration, $r_m = 0.098 \pm 0.003$, was also calculated with the same fitting function (Figure 8). Similar experiments were performed at 2.0 and 5.5 M GdHCl. All the data are reported in Figure 9a.

The dissociation was also monitored using dynamic fluorescence. In particular, the width of the lifetime distribution is very sensitive to the dissociation process (Figure 9b), while the center of the distribution is not affected by the protein concentration (data not shown).

DISCUSSION

Protein Stability. Crystallographic and calorimetric studies on HSOD (Parge et al., 1986; Biliaderis et al., 1987) have demonstrated that this dimeric enzyme is very stable and that Cu and Zn ions play a relevant role in keeping the native structure. HSOD, like the homologous bovine enzyme, is structured into domains connected by hydrophobic, electrostatic, and covalent bonds (Getzoff et al., 1989; Tainer et al., 1982). In agreement with these data, we have demonstrated that 6 M GdHCl is required to unfold holo-HSOD while a lower concentration (3.5 M) is needed to unfold the metal-depleted form, as detected by steady-state fluorescence and anisotropy measurements. The effect of GdHCl on the protein structure may also be monitored by anisotropy decay measurements. In particular, information about the shape of the macromolecule can be obtained from the long rotational correlation time. This parameter decreases very quickly above 1 M GdHCl, suggesting that a loosening of the protein in the dimeric form may occur beyond this concentration. Furthermore, the presence or absence of the metals affects the rotational lifetime of native HSOD while the unfolded samples show similar values (Table I). This result suggests that the metals may influence the tryptophan mobility, making the protein molecule more rigid. A comparison of fluorescence and CD data confirms this hypothesis. Two experimental evidences show that the removal of metals modifies the mobility of the tryptophan-containing domain but not the secondary structure of the protein. First, the CD spectra of holo- and apoprotein samples have the same minimum at ≈210 nm. Second, the same amount of GdHCl is required to destroy completely the secondary structure of both protein forms (Figure 5) while apo-HSOD and holo-HSOD show transitions monitored by fluorescence at different denaturant concentrations, respectively.

Heterogeneity of the Tryptophan Microenvironment. A protein can be considered a complex physical system fluctuating among a large number of similar conformational substates (Austin et al., 1975). In particular, both local and global small motions have been discussed in terms of interconverting processes among substates (Ansari et al., 1985; Hong et al., 1990). The time scale of interconversion is characteristic for each protein and is affected by the same factors that influence the stability of the macromolecular structure (i.e., temperature, pH, denaturants). We would like to suggest that the width of the lifetime distribution recovered from the fit of the fluorescence decay data indeed reflects the number of protein conformational substates and/or the fluctuations of the protein. This hypothesis for HSOD can be defended on the basis of the following observations.

First, let us consider the ratio between the widths of apo- and holo-HSOD in buffer. This ratio is about 1.6, suggesting that the heterogeneity of the fluorophore microenvironment is greater in the metal-depleted molecule, as expected on the basis of structural considerations. This is further confirmed by the broader peak of sedimentation of apo-HSOD observed in the analytical ultracentrifugation experiments (Figure 6a) and by the difference in rotational correlation times (Table I).

Second, the unfolded state is always characterized by a distribution of lifetimes broader than that of native state (Figure 3b). This finding suggests that the fluorophore experiences a larger number of environments in the unfolded state because of the loss of a defined three-dimensional structure.

Insights into the Denaturation Mechanism of HSOD. The denaturation mechanism of a protein can be described either as a two-state process or as a multistate process. The former hypothesis requires that only the folded and the completely unfolded conformations are present in solution during the denaturation process. This model has been extensively developed in the case of small globular proteins (Privalov, 1979) for which a simple sigmoidal transition curve should be expected. On the other hand, the multistate model requires the presence of at least an intermediate form sometimes described as a "molten globule" (Ptitsyn et al., 1990). In the case of HSOD, the data reported above indicate a more complicated denaturation mechanism.

First, the dependence of the width of the lifetime distribution on the denaturant concentration cannot be explained in terms of folded and unfolded molecules only. In fact, if the fluorescence decay at each denaturant concentration is fitted by the sum of two distributions (corresponding to native and

Table I: Anisotropy Decay Parameters[a]

sample	one rotation			two rotations					
	χ^2	Φ	r_0	χ^2	Φ_1	Φ_2	r_1	r_2	r_0
holo-HSOD	3.9	16.6	0.23	2.0	15.9	0.09	0.22	0.06	0.28
apo-HSOD	2.8	11.9	0.22	2.2	13.8	0.16	0.21	0.07	0.28
holo + 6.5 M GdHCl	7.9	1.2	0.20	1.3	3.7	0.40	0.13	0.15	0.28
apo + 3.0 M GdHCl	10.2	1.6	0.15	3.5	4.1	0.22	0.07	0.21	0.28

[a] Φ, Φ_1, and Φ_2, rotational correlation times in nanoseconds ($\delta\Phi$, $\delta\Phi_1 \approx \pm 0.5$ ns; $\delta\Phi_2 \approx \pm 0.03$ ns). r_0, r_1, and r_2, zero-time anisotropies ($\delta r \approx \pm 0.02$). χ^2, reduced χ^2.

Table II: Fluorescence Decay Parameters of Holo-HSOD in GdHCl

GdHCl (M)	one Lorentzian fit[a]			two fixed Lorentzians fit[b]	
	χ^2	C	W	χ^2	F_1
0.0	1.3	2.20	0.40	1.3	1.00
1.0	1.6	1.99	0.39	1.8	1.00
2.0	1.6	2.07	0.44	5.5	0.92
3.0	1.4	2.21	0.59	10.8	0.89
4.0	2.5	2.49	0.82	17.9	0.71
4.5	1.9	2.84	0.90	8.8	0.40
5.0	1.6	3.13	0.81	2.6	0.17
6.0	1.4	3.28	0.67	2.4	0.04
6.5	1.6	3.35	0.68	1.6	0.00

[a] Phase and modulation data are fitted with a single Lorentzian-shaped continuous distribution of lifetimes. (C = center of Lorentzian in nanoseconds, $\delta C \approx 0.02$ ns; W = width of Lorentzian in nanoseconds, $\delta W \approx 0.03$ ns). [b] Phase and modulation data are fitted with the sum of the Lorentzian relative to the native protein (L_1, C_1 = 2.20 ns, W_1 = 0.40 ns) plus that relative to the unfolded one (L_2, C_2 = 3.35 ns, W_2 = 0.68 ns). F_1 = fraction of fluorescence relative to L_1. χ^2 = reduced χ^2.

denatured species), the value of the χ^2 is always higher than that obtained with a single Lorentzian fit (Table II). An attempt to take into account a first-order (linear) perturbation due to guanidine gave much higher χ^2 values (data not shown).

Second, HSOD is a dimeric enzyme, and as demonstrated by ultracentrifugation and protein concentration dependent experiments, monomeric species are appearing along the denaturation pathway. These species, whose secondary structure is still that of native molecules, should have peculiar characteristics that can strongly influence the fluorescence emission decay. In fact, the two subunits of HSOD are held together by interactions occurring between two highly hydrophobic regions of the monomers. These regions are completely exposed to the solvent when the dimer splits into halves. Thus, it is not surprising that the tertiary structure of the isolated subunit may be different with respect to the native conformation, inducing a relevant surface tension that affects the tryptophan microenvironment. While the mean lifetime is unchanged upon dilution of the samples, an increase in heterogeneity of the fluorescence decay is shown by the broadening of the distribution. The transition is shifted to higher protein concentrations by increasing the amount of denaturant (Figure 9b).

As the CD signal at 3.5 M GdHCl is nearly two-thirds that of the native sample (Figure 5, inset), one should assume that part of the molecules are already unfolded at this denaturant concentration. On the other hand, we have shown that no further decrease of the CD signal is observed upon diluting the sample and therefore the fraction of unfolded molecules is not increased.

Kinetic data on this denaturation process (Figure 7) confirmed the complexity of the system, because any attempt to fit these data with simple one- or two-step mechanisms was unsuccessful.

These data, together with previous observations on the stability of the protein and the presence of multiple subconformations also in the native state, allowed us to establish a model for the unfolding mechanism of HSOD. According to this model, the addition of increasing amounts of GdHCl to the protein shifts the monomer–dimer equilibrium toward the monomers. At the same time, due to the surface tension driven by hydrophobic interactions, some of the monomers (i.e., the most unstable species) collapse to the completely unfolded forms. Overall, the following reactions take place:

$$[D] \leftrightarrow 2[M] \rightarrow 2[U]$$

where [U] represents the concentration of unfolded molecules. It should be noted that the second step may also occur at low denaturant concentration in parallel with the dimer dissociation. This effect does not allow us to isolate the two processes.

The instability of some monomeric species is clearly the most relevant feature of this mechanism. In fact, it suggests an explanation for the wide occurrence of oligomeric proteins in biological systems. The rationale of quaternary structure in nonallosteric proteins would be the stabilization of the conformation of the subunits in a more rigid and compact system.

ACKNOWLEDGMENT

We thank Prof. William H. Bannister, University of Malta, for the kind gift of some human superoxide dismutase and Prof. Paola Vecchini, University of Rome "La Sapienza", for the ultracentrifuge experiments. Part of the experiments and data analysis described in this paper were performed at the Laboratory for Fluorescence Dynamics (LFD) at the University of Illinois at Urbana–Champaign (UIUC).

REFERENCES

Alcala, R., Gratton, E., & Prendergast, F. (1987a) *Biophys. J. 51*, 587–596.

Alcala, R., Gratton, E., & Prendergast, F. (1987b) *Biophys. J. 51*, 597–604.

Alcala, R., Gratton, E., & Prendergast, F. (1987c) *Biophys. J. 51*, 925–936.

Ansari, A., Berendzen, S., Bowne, S. F., Frauenfelder, H., Iben, I. E., Sanke, T. B., Shymsunder, E., & Young, R. (1985) *Proc. Natl. Acad. Sci. U.S.A. 82*, 5000–5004.

Austin, R. H., Beeson, K. W., Eisenstein, L., Frauenfelder, H., & Gunsalus, I. C. (1975) *Biochemistry 14*, 5355–5373.

Bannister, J. V., & Bannister, W. H. (1984) *Methods Enzymol. 105*, 88–93.

Beechem, J. M., & Brand, L. (1985) *Annu. Rev. Biochem. 54*, 43–71.

Beechem, J. M., & Gratton, E. (1988) *Proc. SPIE—Int. Soc. Opt. Eng. 909*, 70–81.

Biliaderis, C. G., Weselake, R. J., Petkau, A., & Friesen, A. D. (1987) *Biochem. J. 248*, 981–984.

Bismuto, E., Gratton, E., & Irace, G. (1988) *Biochemistry 27*, 2132–2136.

Creighton, T. E. (1978) *Prog. Biophys. Mol. Biol. 33*, 231–297.

Dolgikh, D. A., Gilmanshin, R. I., Brazhnikov, E. V., Bychkova, V. E., Semisotnov, G. V., Venyaminov, S. Yu., & Ptitsyn, O. B. (1981) *FEBS Lett. 136*, 311–315.
Dolgikh, D. A., Kolomiets, A. P., Bolotina, I. A., & Ptitsyn, O. B. (1984) *FEBS Lett. 165*, 88–92.
Forman, H. J., & Fridovich, I. (1973) *J. Biol. Chem. 248*, 2645–2649.
Getzoff, E. D., Tainer, J. A., Stempien, M. M., Bell, G. I., & Hallewell, R. A. (1989) *Proteins: Struct., Funct., Genet. 5*, 322–336.
Gratton, E., & Limkeman, M. (1983) *Biophys. J. 44*, 315–324.
Gratton, E., Jameson, D. M., & Hill, R. (1984) *Annu. Rev. Biophys. Bioeng. 13*, 105–124.
Gryczynski, I., Eftink, M., & Lakowicz, J. R. (1988) *Biochim. Biophys. Acta 954*, 244–252.
Holladay, L. A., Hammonds, R. G., Jr., & Puett, D. (1974) *Biochemistry 13*, 1653–1661.
Hong, M. K., Braunstein, D., Cowen, B. R., Frauenfelder, H., Iben, I. E. T., Mourant, J. R., Ormos, P., Scholl, R., Schulte, A., Steinbach, P. J., Xie, A. H., & Young, R. D. (1990) *Biophys. J. 58*, 429–436.
Jaenicke, R. (1991) *Biochemistry 30*, 3147–3161.
James, D. R., Dremer, D. R., Steer, R. P., & Veral, R. E. (1985) *Biochemistry 24*, 5517–5526.
Karplus, M., & Petsko, G. A. (1990) *Nature 347*, 631–639.
Kim, P. S., & Baldwin, R. L. (1982) *Annu. Rev. Biochem. 51*, 459–489.
Kuwajima, K. (1977) *J. Mol. Biol. 114*, 241–258.
Kuwajima, K. (1989) *Proteins: Struct. Funct., Genet. 6*, 87–103.
Lakowicz, J. R., Cherek, H., Gryczynski, I., Joshi, N., & Johnson, M. L. (1987) *Biophys. Chem. 28*, 35–50.
Libertini, L. J., & Small, E. W. (1989) *Biophys. Chem. 34*, 269–282.
Malinowski, D. P., & Fridovich, I. (1979) *Biochemistry 18*, 5055–5060.
Munro, I., Pecht, I., & Stryer, L. (1979) *Proc. Natl. Acad. Sci. U.S.A. 76*, 56–60.
Pace, C. N. (1986) *Methods Enzymol. 131*, 266–280.
Parge, H. E., Getzoff, E. D., Scandella, C. S., Hallewell, R. A., & Tainer, J. A. (1986) *J. Biol. Chem. 261*, 16215–16218.
Privalov, P. L. (1979) *Adv. Protein Chem. 33*, 167–241.
Ptitsyn, O. B., Pain, R. H., Semisotnov, G. V., Zerovnik, E., & Razgulyaev, O. (1990) *FEBS Lett. 262*, 20–24.
Rosato, N., Gratton, E., Mei, G., & Finazzi-Agrò, A. (1990a) *Biophys. J. 58*, 817–822.
Rosato, N., Mei, G., Gratton, E., Bannister, J. V., Bannister, W. H., & Finazzi-Agrò, A. (1990b) *Biophys. Chem. 36*, 41–46.
Tainer, J. A., Getzoff, E. D., Beem, K. M., & Richardson, D. C. (1982) *J. Mol. Biol. 160*, 181–217.
Weber, G. (1953) *Adv. Protein Chem. 8*, 415–459.

Registry No. SOD, 9054-89-1; Cu, 7440-50-8; Zn, 7440-66-6.